Airborne Observations and Modeling Comparison of Global Inorganic Aerosol Acidity

Get Data

Documentation Revision Date: 2022-03-17

Dataset Version: 1

Summary

This dataset provides observations collected during eleven airborne campaigns from 2006–2017 and associated input and output from nine widely used chemical transport models (CTMs). The airborne campaigns include ARCTAS-A, ARCTAS-B, ATom-1 and ATom-2, CalNex, DC3, INTEX-B, KORUS-AQ, MILAGRO, SEAC4RS, and WINTER, and they sampled mainly tropospheric air over the conterminous U.S. and the state of Alaska, Mexico, Canada, Greenland, and South Korea and remote areas over the Arctic, Pacific, Southern, and Atlantic Oceans. The CTMs are the AM4.1, CCSM4, GEOS-5, GEOS-Chem TOMAS, GEOS-Chem v10, GEOS-Chem v12, GISS-MATRIX, GISS-ModelE, and TM4-ECPL-F, and the output includes sulfate, nitrate, temperature, specific humidity, mixing ratio of ammonium, the volume mixing ratio of nitric acid, surface pressure, gas-phase ammonia, gas-phase nitric acid, pressure, total ammonium, etc. The observations were collected in-situ from a variety of instruments, including the Aerosol Microphysical Properties (AMP), HR Aerodyne Aerosol Mass Spectrometer (AMS), CIT Chemical Ionization Mass Spectrometer (CIMS), diode laser hygrometer (DLH), a mist chamber/ion chromatography system (MC/IC), Particle Analysis by Laser Mass Spectrometer (PALMS), Single Particle Soot Photometer (SP2), and UCI Whole Air Sampler (WAS). In-situ data also include latitude, longitude, and pressure. These observations were used to investigate how aerosol pH and ammonium balance change from polluted to remote regions, such as over oceans, and were compared to predictions from the CTMs.

There are 63 total data files included in this dataset; 53 in netCDF (*.nc) format and 10 in Hierarchical Data (HDF; *.h5) format. Also included are two companion files in Portable Document (*.pdf) formats.

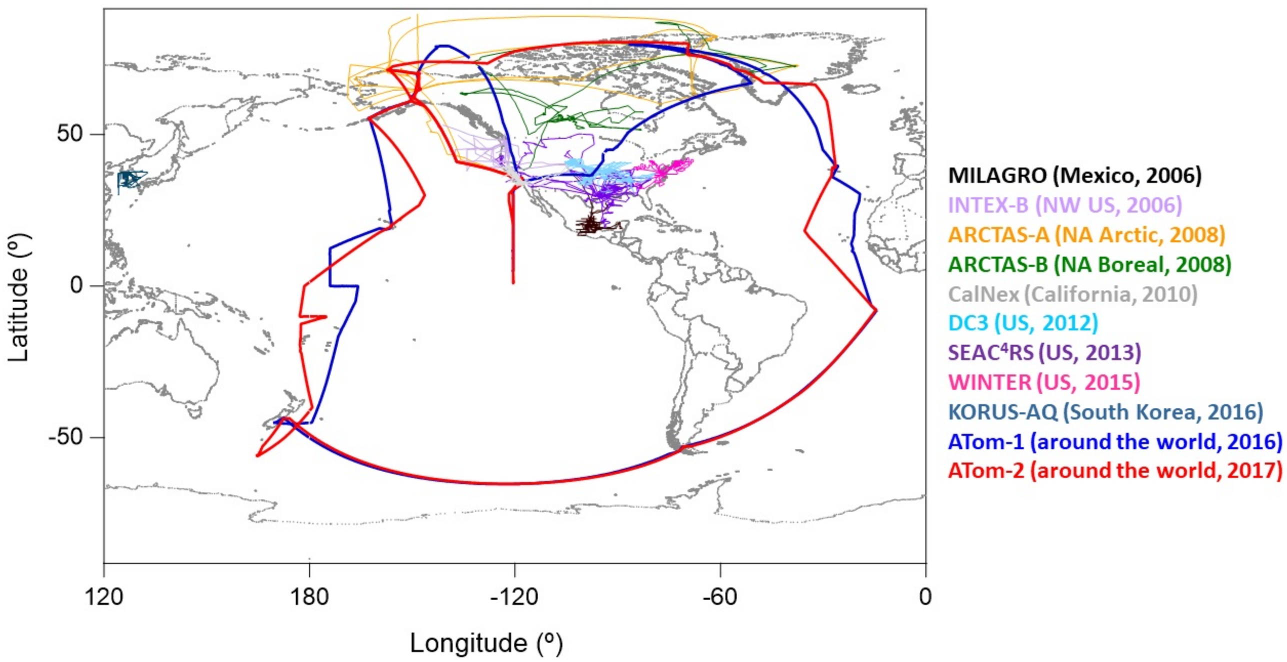

Figure 1. Flight tracks for airborne campaigns in this dataset.

Citation

Nault, B.A., P. Campuzano-Jost, D.A. Day, D.S. Jo, J.C. Schroder, H.M. Allen, R. Bahreini, H. Bian, D.R. Blake, M. Chin, S.L. Clegg, P.R. Colarco, J.D. Crounse, M.J. Cubison, P.F. Decarlo, J.E. Dibb, G.S. Diskin, A. Hodzic, W. Hu, J.M. Katich, J.K. Kodros, A. Kupc, F.D. Lopez-Hilfiker, E.A. Marais, A.M. Middlebrook, J.A. Neuman, J.B. Nowak, B.B. Palm, F. Paulot, J.R. Pierce, G.P. Schill, E. Scheuer, J.A. Thornton, K. Tsigaridis, P.O. Wennberg, C.J. Williamson, and J.L. Jimenez. 2022. Airborne Observations and Modeling Comparison of Global Inorganic Aerosol Acidity. ORNL DAAC, Oak Ridge, Tennessee, USA. https://doi.org/10.3334/ORNLDAAC/1857

Table of Contents

1. Dataset Overview
2. Data Characteristics
3. Application and Derivation
4. Quality Assessment
5. Data Acquisition, Materials, and Methods
6. Data Access
7. References

1. Dataset Overview

This dataset provides observations collected during eleven airborne campaigns from 2006–2017 and associated input and output from nine widely used chemical transport models (CTMs). The airborne campaigns include ARCTAS-A, ARCTAS-B, ATom-1 and ATom-2, CalNex, DC3, INTEX-B, KORUS-AQ, MILAGRO, SEAC4RS, and WINTER, and they sampled mainly tropospheric air over the conterminous U.S. and the state of Alaska, Mexico, Canada, Greenland, and South Korea and remote areas over the Arctic, Pacific, Southern, and Atlantic Oceans. The CTMs are the AM4.1, CCSM4, GEOS-5, GEOS-Chem TOMAS, GEOS-Chem v10, GEOS-Chem v12, GISS-MATRIX, GISS-ModelE, and TM4-ECPL-F, and the output includes sulfate, nitrate, temperature, specific humidity, mixing ratio of ammonium, volume mixing ratio of nitric acid, surface pressure, gas-phase ammonia, gas-phase nitric acid, pressure, total ammonium, etc. The observations were collected in-situ from a variety of instruments, including the Aerosol Microphysical Properties (AMP), HR Aerodyne Aerosol Mass Spectrometer (AMS), CIT Chemical Ionization Mass Spectrometer (CIMS), diode laser hygrometer (DLH), a mist chamber/ion chromatography system (MC/IC), Particle Analysis by Laser Mass Spectrometer (PALMS), Single Particle Soot Photometer (SP2), and UCI Whole Air Sampler (WAS). In-situ data also include latitude, longitude, and pressure. These observations were used to investigate how aerosol pH and ammonium balance change from polluted to remote regions, such as over oceans, and were compared to predictions from the CTMs.

Project: Atmospheric Tomography Mission

The Atmospheric Tomography Mission (ATom) is a NASA Earth Venture Suborbital-2 mission to study the impact of human-produced air pollution on greenhouse gases and on chemically reactive gases in the atmosphere. ATom deployed an extensive gas and aerosol payload on the NASA DC-8 aircraft for a systematic, global-scale sampling of the atmosphere, profiling continuously from 0.2 to 12 km altitude. Around-the-world flights were conducted in each of four seasons between 2016 and 2018.

Related Publication

Nault, B.A., P. Campuzano-Jost, D.A. Day, D.S. Jo, J.C. Schroder, H.M. Allen, R. Bahreini, H. Bian, D.R. Blake, M. Chin, S.L. Clegg, P.R. Colarco, J.D. Crounse, M.J. Cubison, P.F. DeCarlo, J.E. Dibb, G.S. Diskin, A. Hodzic, W. Hu, J.M. Katich, M.J. Kim, J.K. Kodros, A. Kupc, F.D. Lopez-Hilfiker, E.A. Marais, A.M. Middlebrook, J. Andrew Neuman, J.B. Nowak, B.B. Palm, F. Paulot, J.R. Pierce, G.P. Schill, E. Scheuer, J.A. Thornton, K. Tsigaridis, P.O. Wennberg, C.J. Williamson, and J.L. Jimenez. 2021. Chemical transport models often underestimate inorganic aerosol acidity in remote regions of the atmosphere. Communications Earth & Environment 2:93. https://doi.org/10.1038/s43247-021-00164-0

Related Datasets

Allen, H.M., J.D. Crounse, M.J. Kim, A.P. Teng, and P.O. Wennberg. 2019. ATom: L2 In Situ Data from Caltech Chemical Ionization Mass Spectrometer (CIT-CIMS). ORNL DAAC, Oak Ridge, Tennessee, USA. https://doi.org/10.3334/ORNLDAAC/1713

Barletta, B., B.C. Biggs, D.R. Blake, N. Blake, A. Hoffman, S. Hughes, et al. 2019. ATom: L2 Halocarbons and Hydrocarbons from the UC-Irvine Whole Air Sampler (WAS). ORNL DAAC, Oak Ridge, Tennessee, USA. https://doi.org/10.3334/ORNLDAAC/1751

Brock, C.A., A. Kupc, C.J. Williamson, K. Froyd, F. Erdesz, D.M. Murphy, et al. 2019. ATom: L2 In Situ Measurements of Aerosol Microphysical Properties (AMP). ORNL DAAC, Oak Ridge, Tennessee, USA. https://doi.org/10.3334/ORNLDAAC/1671

Dibb, J.E. 2019. ATom: Measurements of Soluble Acidic Gases and Aerosols (SAGA). ORNL DAAC, Oak Ridge, Tennessee, USA. https://doi.org/10.3334/ORNLDAAC/1748

Jimenez, J.L., P. Campuzano-Jost, D.A. Day, B.A. Nault, D.J. Price, and J.C. Schroder. 2019. ATom: L2 Measurements from CU High-Resolution Aerosol Mass Spectrometer (HR-AMS). ORNL DAAC, Oak Ridge, Tennessee, USA. https://doi.org/10.3334/ORNLDAAC/1716

Schwarz, J.P., and J.M. Katich. 2019. ATom: L2 In Situ Measurements from Single Particle Soot Photometer (SP2). ORNL DAAC, Oak Ridge, Tennessee, USA. https://doi.org/10.3334/ORNLDAAC/1672

Williamson, C.J., A. Kupc, K.R. Bilsback, T.P. Bui, P.C. Jost, M. Dollner, K.D. Froyd, A.L. Hodshire, J.L. Jimenez, J.K. Kodros, G. Luo, D.M. Murphy, B.A. Nault, E. Ray, B. Weinzierl, F. Yu, P. Yu, J.R. Pierce, and C.A. Brock.. 2019. ATom: In Situ Tropical Aerosol Properties and Comparable Global Model Outputs. ORNL DAAC, Oak Ridge, Tennessee, USA. https://doi.org/10.3334/ORNLDAAC/1684

Wofsy, S.C., and ATom Science Team. 2018. ATom: Aircraft Flight Track and Navigational Data. ORNL DAAC, Oak Ridge, Tennessee, USA. https://doi.org/10.3334/ORNLDAAC/1613

Acknowledgments

This work was supported by NASA's ATom project (grant NNX15AH33A), NASA's Airborne Research (grant NNX15AJ23G and NNX15AG61A), NASA's AMS Quantification (grant 80NSSC19K0124), NASA's FIREX-AQ (grant 80NSSC18K0630), the National Science Foundation (grant 1360745 and 1652688), and the Department of Energy BER/ASR Program (grant DE-SC0016559).

2. Data Characteristics

Spatial Coverage: approximately 80 N to 70 S (i.e., from South Korea/Mid Pacific eastward to mid-Atlantic, including Arctic Ocean, Southern Ocean, and North American continent)

Spatial Resolution: varies across files

Temporal Coverage: 2006-01-01 to 2017-01-01 for observation, varies for CTMs

Temporal Resolution: 1-minute for observations, monthly for CTMs

Study Area: Latitude and longitude are given in decimal degrees.

Site	Northernmost Latitude	Southernmost Latitude	Easternmost Longitude	Westernmost Longitude
Global	90	-90	180	-180

Data File Information

There are 63 total data files included in this dataset; 53 in netCDF (*.nc) format and 10 in Hierarchical Data (HDF; *.h5) format. Also included are two companion files in Portable Document (*.pdf) format: one is a copy of this user guide and the other provides the names of each file according to its grouping (see Table 1). The file names do not have a consistent naming convention.

Table 1. File groupings and descriptions. All files are in netCDF format, except for AM4.1 which uses HDF format. The file names are listed for each grouping in the companion file file_groupings.pdf. Values for CTMs (i.e., all groupings except for observations) are global monthly averages for 12 months.

File Grouping	Number of Files	Description	Reference
AM4.1	10	HDF files. Variables (and corresponding file names) include aerosol pH (aerosol_ph), gas-phase nitric acid (hno3), gas-phase ammonia (nh3), total ammonium (nh4), total ammonium nitrate (nh4no3), sulfate (so4), surface pressure (ps), specific humidity (sphum), temperature (temp), and pressure (static).	Horowitz et al., 2020
CCSM4	7	Variables (and corresponding file names) include specific humidity (hus), mixing ratio of ammonium (mmrnh4), nitrate (mmrno3), sulfate (mmrso4), surface pressure (ps), temperature (temp), volume mixing ratio of nitric acid (vmrhno3).	Tsigaridis et al., 2014
GEOS-5	9	Variables (and corresponding file names) include specific humidity (hus), mixing ratio of ammonium (mmrnh4), nitrate (mmrno3), and sulfate (mmrso4), relative humidity (rh), air density (rho), temperature (ta), and volume mixing ratio of nitric acid (hno3) and ammonia (nh3).	Bian et al., 2017
GEOS-Chem TOMAS	1	Variables include gas-phase nitric acid, gas-phase ammonia, ammonium, nitrate (variable *NIT*), sulfate, specific humidity (variable *SPHU*), temperature, and pressure.	Kodros & Pierce, 2017
GEOS-Chem v10	1	Variables include gas-phase nitric acid, gas-phase ammonia, ammonium, nitrate, sulfate, pressure (variable *p-edge*), and aerosol pH.	Marais et al., 2016
GEOS-Chem v12	3	Contains the same variables as GEOSChem v10. The following are different between the three models as designated by the file name: "results" has Sea Salt removed from ISORROPIA, "results_include_SeaSalt" has no modifications, and "results_with_OceanicNH3" has updated oceanic ammonia emissions.	Jo et al., 2019
GISS-MATRIX	7	Variables (and corresponding file names) include specific humidity (hus), mixing ratio of ammonium (mmrnh4), nitrate (mmrno3), and sulfate (mmrso4), surface pressure (ps), temperature (temp), and the volume mixing ratio of nitric acid (vmrhno3).	Tsigaridis et al., 2014
GISS-ModelE	7	Variables (and corresponding file names) include specific humidity (hus), mixing ratio of ammonium (mmrnh4), nitrate (mmrno3), and sulfate (mmrso4), surface pressure (ps), temperature (temp), and the volume mixing ratio of nitric acid (vmrhno3).	Tsigaridis et al., 2014
TM4-ECPL-F	7	Variables (and corresponding file names) include the mixing ratio of ammonium (mmrnh4), nitrate (mmrno3), and sulfate (mmrso4), surface pressure (ps), temperature (temp), the volume mixing ratio of nitric acid (vmrhno3), and ammonia (vmrnh3).	Tsigaridis et al., 2014
observations	11	Observations from 11 airborne campaigns (Table 2). The data are at 1-minute temporal resolution and the total temporal coverage spans 2006-03 to 2017-03. The vertical spatial coverage ranges from near-surface (i.e., 50–300 m above ground) to ~12 km. The date and time (in seconds from 1904-01-01), latitude, longitude, static air pressure, and air temperature are included for each measurement.	See Table 2

Data File Details

The Coordinate Reference System is "WGS 84" (EPSG:4326).

Table 2. File names and descriptions for observations. The file names are listed for each observation in the companion file file_groupings.pdf. References that describe the associated campaigns are included.

Airborne Campaign	Description
ARCTAS-A	A single netCDF file for the ARCTAS-A campaign that includes E-AIM input of nitric acid from CIMS; nitric acid from MC/IC; ammonium, nitrate, and sulfate from AMS; and partial water pressure. E-AIM output includes ammonia; pH from CIMS and AMS; and pH from MC/IC and AMS.
ARCTAS-B	A single netCDF file for the ARCTAS-B campaign that includes the same input and output as the ARCTAS-A file.
ATom-1	A single netCDF file for the ATom-1 campaign that includes the same input and output as the ARCTAS-A file. Additional inputs include methyl nitrate from WAS; the fraction of particles detected as biomass burning aerosol from PALMS; and pyridine from AMS determined from both ions and positive matrix factorization.
ATom-2	A single netCDF for the ATom-2 campaign with the same input and output as ATom-1 with the additional input of black carbon mass concentration from SP2.
CalNex	A single netCDF file for the CalNex campaign that includes E-AIM input of nitric acid and ammonia from CIMS; ammonium, nitrate, and sulfate from AMS; and relative humidity. E-AIM output includes pH from CIMS and AMS; and aerosol liquid water.
DC3	A single netCDF file for the DC3 campaign that includes the same input and output as the ARCTAS-A file.
INTEX-B	A single netCDF file for the INTEX-B campaign that includes E-AIM input of nitric acid from CIMS; ammonium, nitrate, and sulfate from AMS; and relative humidity. E-AIM output includes pH from CIMS and AMS and aerosol liquid water.
KORUS-AQ	A single netCDF file for the KORUS-AQ campaign that includes the same input and output as the ARCTAS-A file.
MILAGRO	A single netCDF file for the MILAGRO campaign that includes the same input and output as the INTEX-B file.
SEAC4RS	A single netCDF file for the SEAC4RS campaign that includes the same input and output as the ARCTAS-A file.
WINTER	A single netCDF file for the WINTER campaign that includes E-AIM input of nitric acid from CIMS; ammonium, nitrate, and sulfate from AMS; and partial water pressure. E-AIM output includes ammonia; pH from CIMS and AMS; and aerosol liquid water.

User Notes

The files were not modified for consistency or to follow CF Conventions. The files were not optimized for use in software like Panoply. To retrieve data, it is recommended that users employ NetCDF utilities from Unidata.

3. Application and Derivation

The inorganic fraction of fine particles affects numerous physicochemical processes in the atmosphere, and there is large uncertainty in its burden and composition due to limited global measurements. This dataset provides observations of inorganic non-refractory submicron particulate matter from eleven different aircraft campaigns used to investigate how aerosol pH and ammonium balance change from polluted to remote regions, such as over oceans. The observations span from very polluted to the most remote regions of the troposphere, both geographically (middle of the Pacific and Atlantic Oceans) and vertically (400–250 hPa or ~7–10 km). Nine widely used CTMs with different degrees of sophistication in their treatment of inorganic aerosols are also provided for comparison to the observations.

4. Quality Assessment

Each of the 11 airborne campaigns (i.e., instruments) and nine CTMs have their own measurements of quality. See Nault et al. (2021) for more information.

5. Data Acquisition, Materials, and Methods

Descriptions of the 11 airborne campaigns are listed in Table 4 and Figure 3. In general, the CalNex, KORUS-AQ, MILAGRO, and WINTER campaigns sampled polluted, urban locations; the ARCTAS-A and ARCTAS-B, DC3, INTEX-B, and SEAC4RS campaigns sampled continental background locations (including some biomass burning sampling for ARCTAS-B and SEAC4RS); and, ATom-1 and ATom-2 and part of INTEX-B sampled remote oceanic background over the Pacific, Southern, Atlantic, and Arctic Oceans.

The primary instruments used for data collection are listed in Figure 4. Other measurements that were used in the analysis from the ATom campaigns include AMP suite of aerosol size spectrometers for particle number concentration, PALMS for fraction of biomass burning, SP2 for black carbon mass concentration, and WAS for methyl nitrate. DLH was used for water vapor to calculate relative humidity and was used in all of the DC-8 campaigns listed.

The agreement between the MC/IC and CIMS varied for each campaign, owing to differences in time response and potential instrument issues at high altitudes because of colder temperatures. Thus, both were used to calculate aerosol pH to investigate (and minimize) potential biases in the calculated aerosol pH.

E-AIM is the thermodynamic model used here to calculate gas-liquid equilibrium in the aqueous aerosol systems and pH for both observations and for CTMs that did not calculate aerosol pH online. The H+ and inorganic aerosol liquid water calculated from E-AIM were used to calculate the aerosol pH for observations and models.

The CTMs are described in Figure 5. For the models, areas encompassing each campaign were averaged for each tropospheric pressure zone. This approach was adopted instead of analyzing the models for the flight path of each campaign to minimize the influence of potential biases on the modeled transport of air masses versus the observations. Further, average monthly model results for the same months as the campaigns were compared. The average results were then used to compare the trends in the modeled ammonium balance and aerosol pH versus inorganic mass concentration. For models that did not calculate aerosol pH online, the outputs from the model were used to calculate the aerosol pH offline with E-AIM. One model, TM4-ECPL-F, lacked the output necessary to calculate aerosol pH. GEOS-Chem v12.1.1 was used to calculate the contribution of sulfate, nitrate, and ammonium to DRE.

Further details can be found in Nault et al. (2021).

Table 3. Common abbreviations and acronyms.

Common Usage	Explanation	Data *
AMP	NOAA Aerosol Microphysical Properties	https://doi.org/10.3334/ORNLDAAC/1671
AMS	High-Resolution Aerodyne Aerosol Mass Spectrometer	https://doi.org/10.3334/ORNLDAAC/1716
ARCTAS	Arctic Research of the Composition of the Troposphere from Aircraft and Satellites	
ATom	Atmospheric Tomography Mission	
CIMS	California Institute of Technology Chemical Ionization Mass Spectrometer	https://doi.org/10.3334/ORNLDAAC/1713
CTMs	Chemical Transport Models	
DAAC	Distributed Active Archive Center	
DLH	NASA Langley Diode Laser Hygrometer	
E-AIM	Extended Aerosol Inorganics Model	
MC/IC	a mist chamber/ion chromatography system	https://doi.org/10.3334/ORNLDAAC/1748
PALMS	NOAA Particle Analysis by Laser Mass Spectrometer	https://doi.org/10.3334/ORNLDAAC/1684
SP2	NOAA Single Particle Soot Photometer	https://doi.org/10.3334/ORNLDAAC/1672
WAS	UC-Irvine Whole Air Sampler	https://doi.org/10.3334/ORNLDAAC/1751

***** Instrument data available from the ORNL DAAC.

Table 4. Sources for the 11 airborne campaign observations and manuscript references that describe the campaigns.

Airborne Campaign	Platform	Source	Reference
ARCTAS-A	NASA DC-8	Chen, Gao. 2020. Arctic Research of the Composition of the Troposphere from Aircraft and Satellites (ARCTAS) NASA Airborne Mission Overview. NASA Langley Atmospheric Science Data Center DAAC. https://doi.org/10.5067/SUBORBITAL/ARCTAS2008/DATA001	Jacob et al., 2010

ARCTAS-B	NASA DC-8	Chen, Gao. 2020. Arctic Research of the Composition of the Troposphere from Aircraft and Satellites (ARCTAS) NASA Airborne Mission Overview. NASA Langley Atmospheric Science Data Center DAAC. https://doi.org/10.5067/SUBORBITAL/ARCTAS2008/DATA001	Jacob et al., 2010
ATom-1	NASA DC-8	Wofsy, S.C., and ATom Science Team. 2018. ATom: Aircraft Flight Track and Navigational Data. ORNL DAAC, Oak Ridge, Tennessee, USA. https://doi.org/10.3334/ORNLDAAC/1613	Hodzic et al., 2020
ATom-2	NASA DC-8	Wofsy, S.C., and ATom Science Team. 2018. ATom: Aircraft Flight Track and Navigational Data. ORNL DAAC, Oak Ridge, Tennessee, USA. https://doi.org/10.3334/ORNLDAAC/1613	Hodzic et al., 2020
CalNex	WP-3D ORION	CalNex Science Team. 2012. WP-SD Data Download. NOAA Earth System Research Laboratory Chemical Sciences Division. https://csl.noaa.gov/groups/csl7/measurements/2010calnex/P3/DataDownload/	Ryerson et al., 2013
DC3	NASA DC-8	Chen, Gao. 2013. DC3 Field Campaign Data from DC-8 aircraft Overview. NASA Langley Atmospheric Science Data Center DAAC. https://doi.org/10.5067/aircraft/dc3/dc8/aerosol-tracegas	Barth et al., 2015
INTEX-B	NSF/NCAR C-130	INTEX-B Science Team. 2011. INTEX-B Satellite data - ICARTT File. NASA Langley Atmospheric Science Data Center DAAC. https://doi.org/10.5067/aircraft/intexb/aerosol-tracegas	Singh et al., 2009
KORUS-AQ	NASA DC-8	Chen, Gao. 2018. KorUS-AQ Airborne Mission Overview. NASA Langley Atmospheric Science Data Center DAAC. https://doi.org/10.5067/suborbital/korusaq/data01	Nault et al., 2018; Jordan et al., 2020
MILAGRO	NSF/NCAR C-130	INTEX-B Science Team. 2011. INTEX-B Satellite data - ICARTT File. NASA Langley Atmospheric Science Data Center DAAC. https://doi.org/10.5067/aircraft/intexb/aerosol-tracegas	Molina et al., 2010
SEAC4RS	NASA DC-8	SEAC4RS Science Team. 2014. SEAC4RS Field Campaign Data - W. NASA Langley Atmospheric Science Data Center DAAC. https://doi.org/10.5067/aircraft/seac4rs/aerosol-tracegas-cloud	Toon et al., 2016
WINTER	NSF/NCAR C-130	WINTER Science Team. 2016. WINTER Data Sets. National Center for Atmospheric Research Earth Observing Laboratory. https://data.eol.ucar.edu/master_lists/generated/winter/	Schroder et al., 2018

Location	Field Campaign	Coordinates Longitude (°)	Latitude (°)	Time Period	Season
Central Mexico	MILAGRO[63]	−102 – −88	16 – 28	04 March 2006 – 29 March 2006	Spring
Western US & Eastern Pacific	INTEX-B[64]	−141 – −118	37 – 54	17 April 2006 – 15 May 2006	Spring
Canada, Alaska, Greenland	ARCTAS-A[65]	−180 – −37	60 – 90	18 March 2008 – 19 April 2008	Spring
Canada, Greenland	ARCTAS-B[65]	−136 – −37	50 – 87	26 June 2008 – 13 July 2008	Summer
California, USA	CalNex[66]	−124 – −115	50 – 87	20 April 2010 – 22 June 2010	Spring
Central & Eastern USA	DC3[67]	−106 – −78	30 – 43	04 May 2012 – 23 June 2012	Spring
USA	SEAC^{4}RS[68]	−126 – −79	19 – 51	02 August 2013 – 22 Sept 2013	Summer
Eastern USA	WINTER[56,69]	−85 – −67	32 – 43	01 Feb 2015 – 15 March 2015	Winter
South Korea	KORUS-AQ[43]	123 – 133	30 – 39	01 May 2016 – 09 June 2016	Spring
ATom >50°	ATom-1 & -2[29]	−150 – 0	>50	29 July 2016 – 23 August 2016; 26 Jan 2017 – 21 Feb 2016	Summer[a] Winter[b]
ATom Pacific 25° – 50°	ATom-1 & -2[29]	−180 – −130	25 – 50	29 July 2016 – 23 August 2016; 26 Jan 2017 – 21 Feb 2016	Summer[a] Winter[b]
ATom Pacific −25° – 25°	ATom-1 & -2[29]	−180 – −130	−25 – 25	29 July 2016 – 23 August 2016; 26 Jan 2017 – 21 Feb 2016	Summer[a] Winter[b]
ATom Pacific −50° – −25°	ATom-1 & -2[29]	−180 – −130	−50 – −25	29 July 2016 – 23 August 2016; 26 Jan 2017 – 21 Feb 2016	Summer[a] Winter[b]
ATom < −50°	ATom-1 & -2[29]	−180 – −30	< −50	29 July 2016 – 23 August 2016; 26 Jan 2017 – 21 Feb 2016	Summer[a] Winter[b]
ATom Atlantic −50° – −25°	ATom-1 & -2[29]	−45 – 0	−50 – −25	29 July 2016 – 23 August 2016; 26 Jan 2017 – 21 Feb 2016	Summer[a] Winter[b]
ATom Atlantic −25° – 25°	ATom-1 & -2[29]	−45 – 0	−25 – 25	29 July 2016 – 23 August 2016; 26 Jan 2017 – 21 Feb 2016	Summer[a] Winter[b]
ATom Atlantic 25° – 50°	ATom-1 & -2[29]	−45 – 0	25 – 50	29 July 2016 – 23 August 2016; 26 Jan 2017 – 21 Feb 2016	Summer[a] Winter[b]

[a]ATom-1 was during boreal summer

[b]ATom-2 was during boreal winter

Figure 3. Campaigns and their sampling locations. Superscripts are defined in Nault et al. (2021) supplemental information.

Campaign	NO_3 Measurement	SO_4 and NH_4 Measurement	NH_3 Measurement	HNO_3 Measurement
MILAGRO	HR-AMS[70,71]	HR-AMS[70,71]	N/A	CF_3O-CIMS[72]
INTEX-B	HR-AMS[70,73]	HR-AMS[70,73]	N/A	CF_3O-CIMS[72]
ARCTAS-A	HR-AMS[70,74] MC/IC[75]	HR-AMS[70,74]	N/A	CF_3O-CIMS[72] MC/IC[75]
ARCTAS-B	HR-AMS[70,74] MC/IC[75]	HR-AMS[70,74]	N/A	CF_3O-CIMS[72] MC/IC[75]
CalNex	c-ToF-AMS[76,77]	c-ToF-AMS[76,77]	Acetone-CIMS[78]	SiF_5^--CIMS[79]
DC3	HR-AMS[70] MC/IC[75]	HR-AMS[70]	N/A	CF_3O-CIMS[72] MC/IC[75]
SEAC^{4}RS	HR-AMS[70] MC/IC[75]	HR-AMS[70]	N/A	CF_3O-CIMS[72] MC/IC[75]
WINTER	HR-AMS[69,70]	HR-AMS[69,70]	N/A	I-CIMS[80]
KORUS-AQ	HR-AMS[43,70] MC/IC[75]	HR-AMS[43,70]	N/A	CF_3O-CIMS[72] MC/IC[75]
ATom-1	HR-AMS[17,29,70] MC/IC[75]	HR-AMS[17,29,70]	N/A	CF_3O-CIMS[72] MC/IC[75]
ATom-2	HR-AMS[17,29,70] MC/IC[75]	HR-AMS[17,29,70]	N/A	CF_3O-CIMS[72] MC/IC[75]

Figure 4. Additional instrument and measurement information. Superscripts are defined in Nault et al. (2021) supplemental information.

Model	pH Calculated on-line/off-line	Model Year	Reference
CCSM4	off-line	01/2006 - 12/2006	Tsigaridis et al.[81]
GISS-MATRIX	off-line	01/2006 - 12/2006	Tsigaridis et al.[81]
GISS-ModelE	off-line	01/2006 - 12/2006	Tsigaridis et al.[81]
TM4-ECPL-F	N/A	01/2006 - 12/2006	Tsigaridis et al.[81]
GEOS-Chem v10	on-line	08/2013-07/2014	Marais et al.[82]
GEOS-Chem v12	on-line	07/2013 - 06/2014	Jo et al.[83]
GEOS-5	off-line	03/2016 - 02/2017	Bian et al.[84]
GEOS-Chem TOMAS	off-line	01/2016 - 12/2016	Kodros and Pierce[85]
AM4.1	on-line	01/2007 - 12/2007	Horowitz et al.[86]

Figure 5. Chemical transport models and associated information. For models that calculated pH online, ISORROPIA v2 was used. Superscripts are defined in Nault et al. (2021) supplemental information.

6. Data Access

These data are available through the Oak Ridge National Laboratory (ORNL) Distributed Active Archive Center (DAAC).

Airborne Observations and Modeling Comparison of Global Inorganic Aerosol Acidity

Contact for Data Center Access Information:

- E-mail: uso@daac.ornl.gov
- Telephone: +1 (865) 241-3952

7. References

Barth, M. C., C. A. Cantrell, W. H. Brune, S. A. Rutledge, J. H. Crawford, H. Huntrieser, L. D. Carey, D. MacGorman, M. Weisman, K. E. Pickering, E. Bruning, B. Anderson, E. Apel, M. Biggerstaff, T. Campos, P. Campuzano-Jost, R. Cohen, J. Crounse, D. A. Day, G. Diskin, F. Flocke, A. Fried, C. Garland, B. Heikes, S. Honomichl, R. Hornbrook, L. G. Huey, J. L. Jimenez, T. Lang, M. Lichtenstern, T. Mikoviny, B. Nault, D. O'Sullivan, L. L. Pan, J. Peischl, I. Pollack, D. Richter, D. Riemer, T. Ryerson, H. Schlager, J. St. Clair, J. Walega, P. Weibring, A. Weinheimer, P. Wennberg, A. Wisthaler, P. J. Wooldridge, and C. Ziegler. 2015. The Deep Convective Clouds and Chemistry (DC3) Field Campaign. Bulletin of the American Meteorological Society 96:1281–1309. https://doi.org/10.1175/BAMS-D-13-00290.1

Bian, H., M. Chin, D. A. Hauglustaine, M. Schulz, G. Myhre, S. E. Bauer, M. T. Lund, V. A. Karydis, T. L. Kucsera, X. Pan, A. Pozzer, R. B. Skeie, S. D. Steenrod, K. Sudo, K. Tsigaridis, A. P. Tsimpidi, and S. G. Tsyro. 2017. Investigation of global particulate nitrate from the AeroCom phase III experiment. Atmospheric Chemistry and Physics 17:12911–12940. https://doi.org/10.5194/acp-17-12911-2017

Hodzic, A., P. Campuzano-Jost, H. Bian, M. Chin, P. R. Colarco, D. A. Day, K. D. Froyd, B. Heinold, D. S. Jo, J. M. Katich, J. K. Kodros, B. A. Nault, J. R. Pierce, E. Ray, J. Schacht, G. P. Schill, J. C. Schroder, J. P. Schwarz, D. T. Sueper, I. Tegen, S. Tilmes, K. Tsigaridis, P. Yu, and J. L. Jimenez. 2020. Characterization of organic aerosol across the global remote troposphere: a comparison of ATom measurements and global chemistry models. Atmospheric Chemistry and Physics 20:4607–4635. https://doi.org/10.5194/acp-20-4607-2020

Horowitz, L. W., V. Naik, F. Paulot, P. A. Ginoux, J. P. Dunne, J. Mao, J. Schnell, X. Chen, J. He, J. G. John, M. Lin, P. Lin, S. Malyshev, D. Paynter, E. Shevliakova, and M. Zhao. 2020. The GFDL Global Atmospheric Chemistry-Climate Model AM4.1: Model Description and Simulation Characteristics. Journal of Advances in Modeling Earth Systems 12:e2019MS002032. https://doi.org/10.1029/2019MS002032

Jacob, D. J., J. H. Crawford, H. Maring, A. D. Clarke, J. E. Dibb, L. K. Emmons, R. A. Ferrare, C. A. Hostetler, P. B. Russell, H. B. Singh, A. M. Thompson, G. E. Shaw, E. McCauley, J. R. Pederson, and J. A. Fisher. 2010. The Arctic Research of the Composition of the Troposphere from Aircraft and Satellites (ARCTAS) mission: design, execution, and first results. Atmospheric Chemistry and Physics 10:5191–5212. https://doi.org/10.5194/acp-10-5191-2010

Jo, D. S., A. Hodzic, L. K. Emmons, E. A. Marais, Z. Peng, B. A. Nault, W. Hu, P. Campuzano-Jost, and J. L. Jimenez. 2019. A simplified parameterization of isoprene-epoxydiol-derived secondary organic aerosol (IEPOX-SOA) for global chemistry and climate models: a case study with GEOS-Chem v11-02-rc. Geoscientific Model Development 12:2983–3000. https://doi.org/10.5194/gmd-12-2983-2019

Jordan, C.E., J.H. Crawford, A.J. Beyersdorf, T.F. Eck, H.S. Halliday, B.A. Nault, L.-S. Chang, J. Park, R. Park, G. Lee, H. Kim, J. Ahn, S. Cho, H.J. Shin, J.H. Lee, J. Jung, D.-S. Kim, M. Lee, T. Lee, A. Whitehill, J. Szykman, M.K. Schueneman, P. Campuzano-Jost, J.L. Jimenez, J.P. DiGangi, G.S. Diskin, B. E. Anderson, R.H. Moore, L.D. Ziemba, M.A. Fenn, J.W. Hair, R.E. Kuehn, R.E. Holz, G. Chen, K. Travis, M. Shook, D.A. Peterson, K.D. Lamb, and J.P. Schwarz. 2020. Investigation of factors controlling PM2.5 variability across the South Korean Peninsula during KORUS-AQ. Elementa: Science of the Anthropocene 8:28. https://doi.org/10.1525/elementa.424

Kodros, J. K., and J. R. Pierce. 2017. Important global and regional differences in aerosol cloud-albedo effect estimates between simulations with and without prognostic aerosol microphysics. Atmospheres 122:4003–4018. https://doi.org/10.1002/2016JD025886

Marais, E. A., D. J. Jacob, J. L. Jimenez, P. Campuzano-Jost, D. A. Day, W. Hu, J. Krechmer, L. Zhu, P. S. Kim, C. C. Miller, J. A. Fisher, K. Travis, K. Yu, T. F. Hanisco, G. M. Wolfe, H. L. Arkinson, H. O. T. Pye, K. D. Froyd, J. Liao, and V. F. McNeill. 2016. Aqueous-phase mechanism for secondary organic aerosol formation from isoprene: Application to the southeast United States and co-benefit of SO2 emission controls. Atmospheric Chemistry and Physics 16:1603–1618. https://doi.org/10.5194/acp-16-1603-2016

Molina, L. T., S. Madronich, J. S. Gaffney, E. Apel, B. de Foy, J. Fast, R. Ferrare, S. Herndon, J. L. Jimenez, B. Lamb, A. R. Osornio-Vargas, P. Russell, J. J. Schauer, P. S. Stevens, R. Volkamer, and M. Zavala. 2010. An overview of the MILAGRO 2006 Campaign: Mexico City emissions and their transport and transformation. Atmospheric Chemistry and Physics 10:8697–8760. https://doi.org/10.5194/acp-10-8697-2010

Nault, B.A., P. Campuzano-Jost, D.A. Day, D.S. Jo, J.C. Schroder, H.M. Allen, R. Bahreini, H. Bian, D.R. Blake, M. Chin, S.L. Clegg, P.R. Colarco, J.D. Crounse, M.J. Cubison, P.F. DeCarlo, J.E. Dibb, G.S. Diskin, A. Hodzic, W. Hu, J.M. Katich, M.J. Kim, J.K. Kodros, A. Kupc, F.D. Lopez-Hilfiker, E.A. Marais, A.M. Middlebrook, J. Andrew Neuman, J.B. Nowak, B.B. Palm, F. Paulot, J.R. Pierce, G.P. Schill, E. Scheuer, J.A. Thornton, K. Tsigaridis, P.O. Wennberg, C.J. Williamson, and J.L. Jimenez. 2021. Chemical transport models often underestimate inorganic aerosol acidity in remote regions of the atmosphere. Communications Earth & Environment 2:93. https://doi.org/10.1038/s43247-021-00164-0

Nault, B. A., P. Campuzano-Jost, D. A. Day, J. C. Schroder, B. Anderson, A. J. Beyersdorf, D. R. Blake, W. H. Brune, Y. Choi, C. A. Corr, J. A. de Gouw, J. Dibb, J. P. DiGangi, G. S. Diskin, A. Fried, L. G. Huey, M. J. Kim, C. J. Knote, K. D. Lamb, T. Lee, T. Park, S. E. Pusede, E. Scheuer, K. L. Thornhill, J.-H. Woo, and J. L. Jimenez. 2018. Secondary organic aerosol production from local emissions dominates the organic aerosol budget over Seoul, South Korea, during KORUS-AQ. Atmospheric Chemistry and Physics 18:17769–17800. https://doi.org/10.5194/acp-18-17769-2018

Ryerson, T. B., A. E. Andrews, W. M. Angevine, T. S. Bates, C. A. Brock, B. Cairns, R. C. Cohen, O. R. Cooper, J. A. de Gouw, F. C. Fehsenfeld, R. A. Ferrare, M. L. Fischer, R. C. Flagan, A. H. Goldstein, J. W. Hair, R. M. Hardesty, C. A. Hostetler, J. L. Jimenez, A. O. Langford, E. McCauley, S. A. McKeen, L. T. Molina, A. Nenes, S. J. Oltmans, D. D. Parrish, J. R. Pederson, R. B. Pierce, K. Prather, P. K. Quinn, J. H. Seinfeld, C. J. Senff, A. Sorooshian, J. Stutz, J. D. Surratt, M. Trainer, R. Volkamer, E. J. Williams, and S. C. Wofsy. 2013. The 2010 California Research at the Nexus of Air Quality and Climate Change (CalNex) field study. Atmospheres 118:5830–5866. https://doi.org/10.1002/jgrd.50331

Schroder, J. C., P. Campuzano-Jost, D. A. Day, V. Shah, K. Larson, J. M. Sommers, A. P. Sullivan, T. Campos, J. M. Reeves, A. Hills, R. S. Hornbrook, N. J. Blake, E. Scheuer, H. Guo, D. L. Fibiger, E. E. McDuffie, P. L. Hayes, R. J. Weber, J. E. Dibb, E. C. Apel, L. Jaeglé, S. S. Brown, J. A. Thornton, and J. L. Jimenez. 2018. Sources and Secondary Production of Organic Aerosols in the Northeastern United States during WINTER. Journal of Geophysical Research: Atmospheres 123:7771–7796. https://doi.org/10.1029/2018JD028475

Singh, H. B., W. H. Brune, J. H. Crawford, F. Flocke, and D. J. Jacob. 2009. Chemistry and transport of pollution over the Gulf of Mexico and the Pacific: spring 2006 INTEX-B campaign overview and first results. Atmospheric Chemistry and Physics 9:2301–2318. https://doi.org/10.5194/acp-9-2301-2009

Toon, O. B., H. Maring, J. Dibb, R. Ferrare, D. J. Jacob, E. J. Jensen, Z. J. Luo, G. G. Mace, L. L. Pan, L. Pfister, K. H. Rosenlof, J. Redemann, J. S. Reid, H. B. Singh, A. M. Thompson, R. Yokelson, P. Minnis, G. Chen, K. W. Jucks, and A. Pszenny. 2016. Planning, implementation, and scientific goals of the Studies of Emissions and Atmospheric Composition, Clouds and Climate Coupling by Regional Surveys (SEAC 4 RS) field mission. Journal of Geophysical Research: Atmospheres 121:4967–5009. https://doi.org/10.1002/2015JD024297

Tsigaridis, K., N. Daskalakis, M. Kanakidou, P. J. Adams, P. Artaxo, R. Bahadur, Y. Balkanski, S. E. Bauer, N. Bellouin, A. Benedetti, T. Bergman, T. K. Berntsen, J. P. Beukes, H. Bian, K. S. Carslaw, M. Chin, G. Curci, T. Diehl, R. C. Easter, S. J. Ghan, S. L. Gong, A. Hodzic, C. R. Hoyle, T. Iversen, S. Jathar, J. L. Jimenez, J. W. Kaiser, A. Kirkevåg, D. Koch, H. Kokkola, Y. H. Lee, G. Lin, X. Liu, G. Luo, X. Ma, G. W. Mann, N. Mihalopoulos, J.-J. Morcrette, J.-F. Müller, G. Myhre, S. Myriokefalitakis, N. L. Ng, D. O'Donnell, J. E. Penner, L. Pozzoli, K. J. Pringle, L. M. Russell, M. Schulz, J. Sciare, Ø. Seland, D. T. Shindell, S. Sillman, R. B. Skeie, D. Spracklen, T. Stavrakou, S. D. Steenrod, T. Takemura, P. Tiitta, S. Tilmes, H. Tost, T. van Noije, P. G. van Zyl, K. von Salzen, F. Yu, Z. Wang, Z. Wang, R. A. Zaveri, H. Zhang, K. Zhang, Q. Zhang, and X. Zhang. 2014. The AeroCom evaluation and intercomparison of organic aerosol in global models. Atmospheric Chemistry and Physics 14:10845–10895. https://doi.org/10.5194/acp-14-10845-2014